PHY480 Project Title

Your registration number

December 5, 2018

Abstract

This LaTeX document serves as a template for the PHY480 Autumn Semester report, which is due for submission by the Friday of week 12. The report should have a short abstract, up to about 200 words long, which summarises the contents of the report.

1 Introduction

2 Literature Review

In order to undertake the project it was necessary to first inform myself of the N-Body problem, and its pertinence in Astrophysical problems. To do this, a literature review was undertaken.

2.1 The N-Body Problem

Consider a system of particles, or Bodies, in a dynamic system. In order to understand how the system will behave, the forces acting on each particle need to be ascertained, as well as how this force varies with time. In very simple systems, namely those involving only two particles, there is often an analytical solution to understand how it will behave. Such as the Bohr model of an atom. However, when multiple particles are introduced, more than three to be specific, the problem is impossible to solve analytically, without making simplifying assumptions[1]. Hence, the N-Body Problem.

To overcome this, the equations of motion governing the system are instead solved numerically. When the problem was first identified In the early 17th century, solving these equations to resolve long term dynamical behaviour was completely unfeasible. Consequently, it wasn't until the advent of computers that N-Body simulations began to proliferate in the Astrophysics community.

2.2 The N-Body Problem in Astrophysics

In Astrophysics the distance scales being considered are often much greater than those at which the electrostatic forces act, let alone the nuclear. As a result, the gravitational force is often the one that needs to be considered. Hence, astrophysical problems that analyse the dynamical effects of gravity dominated systems, are the ideal candidate for N-Body simulations.

The latter stages of star formation is perhaps the smallest scale at which N-Body simulations become useful. In the former stages, particle sizes are very small, leaving millions of particles to account for, hence, fluid mechanics are a more computationally feasible way of modelling them. However, this changes once in the runaway and oligarchic growth stages: The onset of more significant gravitational forces, and decrease in number of bodies sees N-Body simulations become a much more effective method.

E. Kokubo and S. Ida were among the first to utilise showcase this, in their paper *On Runaway Growth of Planetesimals*[1]. They performed 3-D N-body simulations of 3000 equally massive planetesimals, orbiting a central body. The simulations provided conclusive evidence of naturally occurring runaway growth, something only previously inferred by statistical analysis of the coagulation condition[2, 3]. The results confirmed the validity of a statistical approach to demonstrate runaway growth. It also highlighted the disadvantages of the statistical approach in later stages of runaway growth, where the planetesimals are grouped spatially: A statistical approach assumes a homogenous distribution of planetesimals.

---

[1] Such a Rydberg atom in atomic Physics that makes the assumption of a 'Hydrogenic' atom, simplifying the problem to the Bohr model.

Once planetary systems are formed they are far from stable, understanding these instabilities, and how they evolve dynamically are another use for N-body simulations.

One example of such instabilities is our early solar system, and studying the dynamism of this system is an active area of research. Namely, unravelling the mysteries of its structure, such as the existence of the Kuiper Belt and Oort cloud. But also explaining its history, in events such as the Late heavy Bombardment. The Nice model solves all of these, and is an example of how N-body simulations can provide answers to problems requiring more specificity to solve.

The nice model, first hypothesised in 2005[4], describes an event in which the outer gas giants, Uranus and Neptune, undergo considerable migrations. The inner gas giants get into a 1:2 resonance, causing dynamical instabilities in the outer orbits. As a result Neptune is propelled past Uranus, as both planets move to their current positions. These migrations disband an early Kuiper belt, pushing asteroids and planetesimals both into the inner system, and out to its far reaches. Thereby explaining both the Oort Cloud, and the Late Heavy Bombardment.

The principal investigative method used in the 2005 paper was the N-Body simulations of an early solar System. K. Tsiganis et al. performed N-Body simulations of the system, including with it a circumstellar disk of planetesimals, truncated at 30 AU. They found orbital resonances in Jupiter and Saturn, would cause excitations in their orbits, and instabilities in those of Uranus and Neptune. Once relaxed, in 50% of the simulations the system would diverge to its current architecture. Perhaps most importantly, the simulations also reproduced the current eccentricities found in the orbits of the Gas Giants, something previously unexplained by planet formation theories.

This was a very high impact paper; since being published it's been cited 717 times. One of which was the extension of the model, namely, its initial conditions.
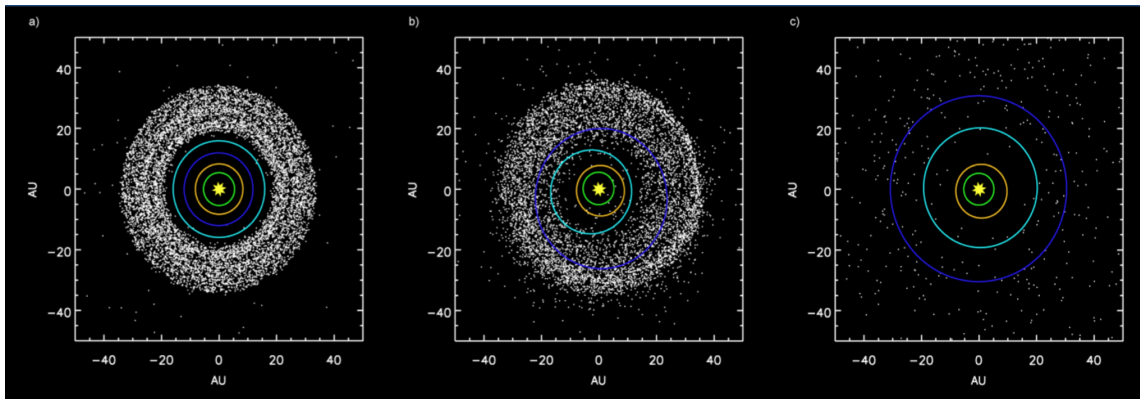

Figure 1: An illustration of the Nice model, with (a) through (c) showing the time evolution of the solar system. It is clear that Uranus (Light Blue) and Neptune (Dark Blue) switch positions in the simulation.

The early solar system is inherently unobservable, hence its initial conditions will always remain a mystery. However, a paper by Batygin et al. aimed to put constraints on the early state of the solar system[5]. They aimed to find *fully resonant* initial conditions, that resulted in the architecture of our current system, post-evolution. Identifying which of these systems evolved in ways that corroborated with the Nice model, was also one of their aims. In their findings they found 4 fully resonant initial conditions that were compatible with the Nice model, and 4 that inferred different evolutions. Their paper explained the importance of multi-resonant in the migration of the planets, and made predictions of the eccentricity jumps and evolutionary paths that given resonances would infer. These hypotheses were then supported using N-Body simulations.

With the Nice model being so well supported by subsequent work, it is now important for future developments to concur with this model.

One such development is the advent of 'Planet 9', not to be confused with Pluto, Planet 9 refers to a planet several earth sizes in mass, orbiting in the far reaches of the solar system. There are many theories that allow for a 9th planet, such as an ejection early in the dynamical timescale of the solar system. A much simpler solution however, would be the capture of a 9th planet from the Sun's birth cluster.

The capture of a 9th planet would be congruent with current theories of the solar system, so long as certain criteria are met, these criteria are detailed at the beginning of a paper by Mustill et al.[6]: The star–star encounter must be at a distance that would not disrupt the Kuiper belt (∼150 AU); The other

star must have a planet on a very wide orbit ($\geqslant$ 100 AU); Lastly, the planet must be captured onto a trajectory that allows for the current orbital distributions of the gas giants. The paper shows, through N-body simulations of star-star encounters, that all of these criteria could be satisfied in a capture event, albeit at a small probability.

In order for a planet to be captured from a foreign star, the sun would likely need to be in a star cluster at the time of capture. These are once again gravitationally dominated systems, and hence the study of their dynamics has been encapsulated by N-body simulations.

The dynamics between stars in clusters, and that of the planets encompassing said stars, are often intertwined physically. This is true to such an extent, that the structure of a protoplanetary system can infer the dynamics of the cluster in which it was formed.

Perturbations will often effect the orbits of young planetary systems, and these perturbations will persist long after the parent cluster has evaporated. The outer orbits of these systems will relax very slowly, and can hence have the potential to carry signatures of their cluster environment. In a paper published by Cai and his colleagues, this hypotheses is supported in detail[7]. They carry out N-body simulations,

N-body simulations were performed of star clusters of varying stellar mass, between 0.04 $M_\odot$ and 25 $M_\odot$. These stars hosted multi-planet systems using two different models, the distribution of semi-major axes remained consistent between these models, starting at 5.2 AU, and extending outwards to $\sim$200 AU. The planetary masses were different in each model, one used Jupiter mass planets, the other $\frac{1}{3}$ Earth mass planets. The dynamical simulations aimed to observe a departure from these initial conditions, these departures arising due to both perturbations from stars, and through planet-planet scattering.

They found that the birth environment of a planetary system can be understood from observed orbital elements. They also suggested that the star clusters cause 'natural selection' between the planetary systems formed within them, where only the most resilient systems would survive. Furthermore, the more dense stellar environments, such as deep inside the cluster, resulted in stronger signatures in the planetary orbits. With these statements they also provided quantitative relationships between the perturbation method, and the inclination and eccentricity of planetary orbits: They found that the inclination and eccentricity would rise systematically when subjected to external perturbations; Or if internal evolution dominated, the inclination would fluctuate in anti-phase with the eccentricity, this mechanism being dominated by the conservation of angular momentum. All of these findings were true regardless of which mass planet was used. These results also allowed the group to hypothesise the Sun's birth environment: The outskirts of a star cluster $\sim$1000 stars in size.

It follows that the reverse is also true, perhaps by observing stars in clusters, you could infer properties of planetary systems encompassing them, by analysing their location in the cluster.

Photometric properties of clusters can be measured from observations, these properties are often used to predict physical parameters such as mass and radii. However, these are often estimations, and to obtain values with certainty, many parameters need to be measured to a high degree of accuracy.

The N-body method sees another use in supporting values estimated using observations, this is shown by H. Baumgardt, in a paper published in 2016[8]. Baumgardt performs 900 N-body simulations of differently initialised star clusters, their concentration, size, and black hole mass fraction were varied between simulations.

By comparing data obtained from observations, against that provided through N-body simulations, the best fitting model was obtained for each cluster. With these models absolute masses could be derived, and hence their mass-light ratios. The presence of black holes in their simulations allowed predictions to be made, regarding the presence of black holes in the observed clusters. Furthermore, cluster distances could be ascertained for galaxies with more accurate velocity dispersion measurements.

They found theoretically predicted mass-light ratios were in strong agreement with those predicted using N-body methods. For the majority of clusters, comparisons with N-body simulations didn't support the existence of black holes. One cluster however, ω Cen, strongly disagreed with N-body models that lacked a large black hole mass fraction, suggesting the cluster hosts a black hole at its centre, the paper suggesting a mass of $\sim$40,000 $M_\odot$.

3   Progress on Project

There are a many ways to approach the N-Body problem to the 4th order. More accurate methods are predictor-correctors, in particular the Hermite Polynomial, and the Adams-Bashforth-Moulton model. The former tries to predict the higher order kinematic components, the aptly named Jerk, Snap, Crack, and Pop. This is computationally expensive, as crossproducts between velocity and acceleration vectors are needed, something relatively inefficient for computer processors to calculate. The Adams-Bashforth-Moulton method predicts future values by fitting a polynomial to previous values, this requires storing previous values of the quantity that needs predicting.

At low values of N, storing these values is more computationally feasible hence, the method is more efficient than the Hermite Method, hence, this project is going to implement the Adams-Bashforth-Moulton model. This method is not self starting, meaning in order to function it requires time-history of the velocity and acceleration vectors. In order to do this, a second order method is necessary to initialise the values used for a time history, in a method known as 'Bootstrapping'. Hence, the first part of the project required implementing an accurate 2nd order N-Body.

3.1   Second order Kinematics

In order to calculate a body's changes in velocity and position over a given time-step, the acceleration vector acting on it must first be calculated. In a system dominated by gravitational forces, this requires knowledge of every body's position in a consistent coordinate system. For a given body, n, its interaction with another body m, can be calculated using Newton's Law of gravitation, provided the distance between them, $\vec{r_{nm}}$, is known. By summing over all interactions the body will have, its total acceleration vector can be calculated as shown in eq. (1).

$$\vec{a_n} = \sum_{m \neq n}^{N} \frac{Gm_m}{|\vec{r_{nm}}|^3} \vec{r_{nm}} \tag{1}$$

Given a discrete time-step over which to apply this acceleration, the changes in distance and velocity can be determined using the kinematic equations. These are shown below, where the subscripts i and f denote the initial and final positions respectively, δt represents the time-step, and $\vec{r}, \vec{v}$ and $\vec{a}$, the position, velocity and acceleration.

$$\vec{r}_{n,f} = \vec{r}_{n,i} + \vec{v}_n \delta t \qquad\qquad\qquad \vec{v}_{n,f} = \vec{v}_{n,i} + \vec{a}_n \delta t$$

For the position, this can easily be extended to the second order, by including the current acceleration. This is shown in eq. (2).

$$\vec{r}_{n,f} = \vec{r}_{n,i} + \vec{v}_n \delta t + \frac{1}{2} \vec{a}_n \delta t^2 \tag{2}$$

To calculate the velocity to the second order, the rate of change of the acceleration is required, the jerk. This is not a simple calculation, and is computationally expensive, hence, an approximation should be made: $\frac{da}{dt} \approx \frac{a_i - a_f}{\delta t}$. Given a small change in acceleration this in a valid assumption. Programatically, this requires storing the previous value of acceleration, a_p. Then by using it in conjunction with the current acceleration, a_c, the second order equation for the velocity can now be taken as eq. (3).

$$\vec{v}_{n,f} \;=\; \vec{v}_{n,i} + \vec{a}_n \delta t + \frac{1}{2} \frac{d\vec{a_n}}{dt} \delta t^2 \;=\; \vec{v}_{n,i} + \vec{a}_{n,c} \delta t + \frac{1}{2}(\vec{a}_{n,p} - \vec{a}_{n,c}) \delta t \tag{3}$$

3.2   Recreating the Solar System accurately

To undertake N-Body simulations, these are the only equations necessary. However, to start the process, initial conditions should be given to each body, namely a mass, position, and velocity. These were taken from a NASA database[9], see appendix A for the values pertinent in this project.

To initialise the simulation, the planets were positioned on the x axis at their orbital radii, and at $y = 0$. Their respective orbital velocities were then applied along the y axis, with $v_x = 0$. Hence, when the simulation was run they would orbit on the x–y plane.

At the beginning of each time-step, the acceleration acting on each body was calculated using eq. (1), this value was then applied to the kinematic equations, eq. (2), and eq. (3). The planets were moved to these positions, and given the corresponding velocities. New accelerations were calculated, and the process was repeated. Since no time history was given, initially the change in acceleration couldn't be calculated in eq. (3). Hence, only the first derivative of velocity was used in the calculation of $\vec{v}_{n,2}$, this was done by manually setting the change in acceleration to zero.

To demonstrate the accuracy of this second order code, a 1000 year simulation of the solar system was carried out with 10 second time-steps. The resulting simulation produced a system with stable orbits, this is reflected in fig. 2. Figure 2 (a) shows the log of orbital distance against time, it is clear the orbits remain at a consistent distance with only Earth drifting very slightly. The oscillations in the distances of Saturn, Uranus, and Neptune, are due to the elliptical nature of their orbits, the eccentricities were reasonable: ~ 0.02, ~ 0.04, and ~ 0.03 respectively. Figure 2 (b) shows the orbits in the x–y plane, demonstrating their circular nature.

(a) Orbital distances against time
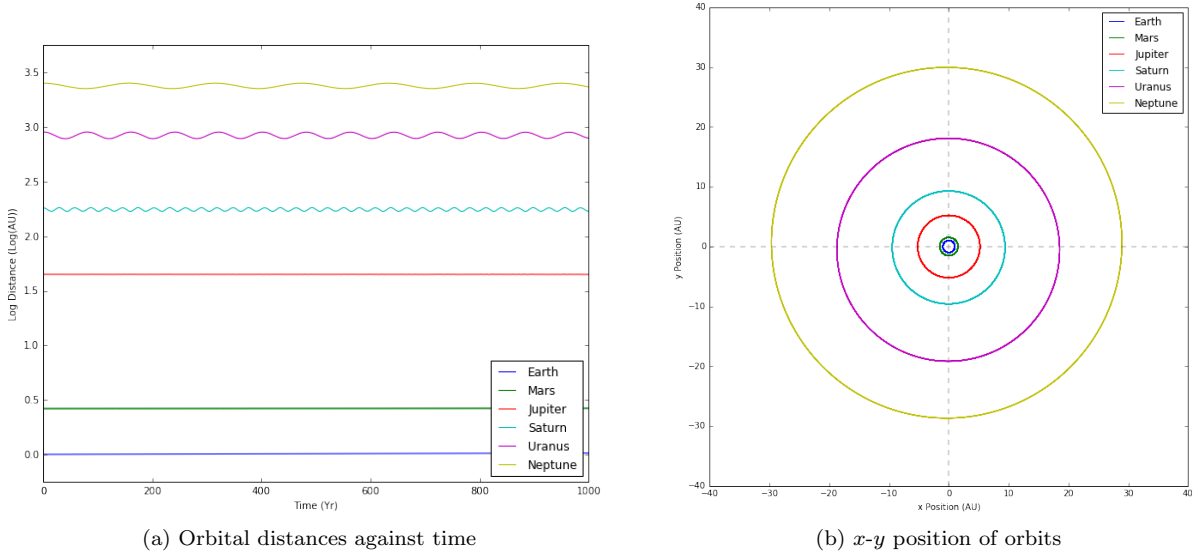
(b) x-y position of orbits

Figure 2: Plots of orbital position throughout the simulation.

To further ensure the model's accuracy, energy conservation was considered. The total energy was calculated when the system was initialised to obtain E_i, this was simply the sum of the kinetic and potential energies, as shown in eq. (4). A factor of a half was applied to the potential energy, as in this summation it would be calculated twice for a given interaction $n \leftrightarrow m$.

$$ E_{tot} = \sum_{n=1}^{N} \left[\frac{1}{2} m_n |v_n|^2 - \sum_{m \neq n}^{N} \frac{G m_m m_n}{2 |r_{nm}|} \right] = \frac{1}{2} \sum_{n=1}^{N} m_n \left[|v_n|^2 - \sum_{m \neq n}^{N} \frac{G m_m}{|r_{nm}|} \right] \tag{4} $$

This value was recalculated throughout the simulation, and compared against the initial value, using eq. (5). Where ΔE, represents the fractional energy loss, and the subscript t denoting the time-step at which the value is calculated.

$$ \Delta E_t = \frac{E_i - E_t}{E_i} \tag{5} $$

This fractional energy loss was plotted against time, to see how it varied throughout the simulation. This is shown in fig. 3. Figure 3 (a) shows the variation across the entire simulation, whereas fig. 3 (b) shows the value over a 100 year time period.

Over the whole simulation, the average energy loss remains close to zero, only lowering slightly, mainly due to the drift of Earth. However, there are clearly oscillatory fluctuations in the value, these oscillations are due to interactions of Jupiter with Saturn. Upon increasing the time-resolution of this graph, fig. 3 (b), smaller scale oscillations can be seen. These are presumably a result of interactions between the other planets in the system. Nonetheless, the energy losses (and its fluctuation) proved to be minor in this simulation; the large scale oscillation having an amplitude of ~ 0.0003, and only lowering by ~ 0.0002.
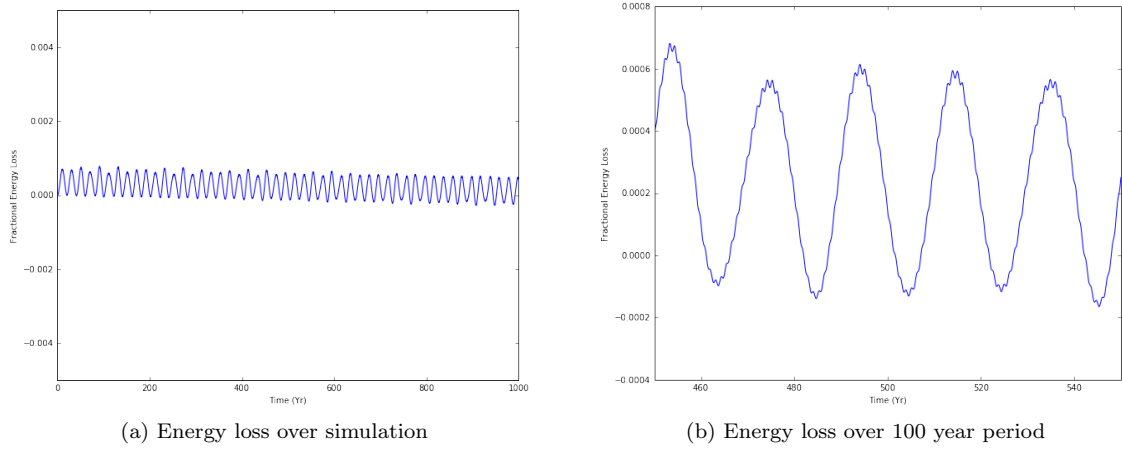
5

(a) Energy loss over simulation

(b) Energy loss over 100 year period

Figure 3: Plots showing the Energy loss throughout the simulation.

3.3 Suitability for Bootstrapping

The previous section demonstrates the code's ability to accurately recreate the orbits of the Solar System, to a reasonable degree of accuracy. However, if a simulation is to run for millions of years, the discrepancies seen in the 2nd order system will manifest as large inaccuracies. Hence, the 4th order Adams-Bashforth-Moulton will be preferred.

As a method of producing the initial time history, the 2nd order code is more than sufficient; over a small timescale, < 80 seconds, the errors seen at long timescales will be infinitesimal. Accordingly, this code will be used initially in the 'bootstrapping' phase.

3.4 Randomising Initial Positions Along Orbit

If the simulation is to be run more than once, it will be beneficial to randomise the initial positions of the planets along their orbit. Should the code be applied to astrophysical problems, this would prevent any deterministic results from arising, thereby producing more natural behaviour.

There are many ways to approach this, some requiring more knowledge of the orbital paths than others. However, with knowledge of the mean orbital radius and velocity, the planet can be placed at any position at a radius equal to the orbital radius. Provided the velocity vector is both perpendicular to the radial vector, and equal to the mean orbital velocity.

Consider the positive quadrant of a planet's orbit (see fig. 2 (b)). On a given axis, the position will take a value between 0 and R, and the velocity will take a value between 0 and v_T, where R and v_T denote the orbital radius and velocity respectively. The component on the other axis can then be calculated using trigonometry. This is represented mathematically as shown in eq. (6), where X_n represents the random number between 0 and 1, assigned to the body, n.

$$r_{x,n} = X_n R_n \qquad \text{and} \qquad v_{y,n} = X_n v_{T,n} \qquad (6)$$

Then by using Trigonometry, the components along the other axes can be calculated, as shown in eq. (7). Note the opposite axis on r_n, and v_n respectively in eq. (6), this is due to the velocity vector being perpendicular to the radius vector.

$$r_{y,n} = R_n^2 - r_{x,n}^2 \qquad \text{and} \qquad v_{x,n} = v_{T,n}^2 - v_{y,n}^2 \qquad (7)$$

To allow for the other three quadrants, a random factor of ± 1 should be applied to each component of the position. The value applied to the velocity will depend on the value applied to the radius vector. That is to say, the quadrant allocated by the random factors of ± 1 will determine the value of ± 1 applied to the velocity components.

This was achieved programatically by first randomly assigning a value of ± 1 to each position vector component, a parity. Then, using a simple series of *IF* statements, the velocity components were allocated

6

parities, thus creating two 1×2 arrays for each quantity. The conditions for the algorithm are illustrated in table 1.

Position [x,y]	Velocity [v_x,v_y]
[1,1]	[-1,1]
[-1,1]	[-1,-1]
[-1,-1]	[1,-1]
[1,-1]	[1,1]

Table 1: Position parity vectors, with corresponding velocity parity vectors.

Regardless of which quadrant they're in, the same trigonometric relations in eq. (7) exist between the quantities, and their components. Hence, with a random number allocated to each position component, the planet can be randomly positioned in any quadrant, and in any position along its orbit.

This functionality was added to the code, and the resultant behaviour was identical to that seen in fig. 2 and fig. 3.

3.5 Moving Forward

As section 3.3 states, this code will be more than sufficient for initialising the first 8 time-steps of a predictor-corrector. Furthermore, with planets being positioned at completely random positions along their orbit, there is no chance of a deterministic effects arising from the initial setup of the system.

Hence, the project can continue towards the goal of creating a 4th Order Predictor Corrector. The logistics of this are detailed in the next section.

4 Project Plan

References

[1] Kokubo, E., and S. Ida
On Runaway growth of Planetesimals: N-body simulation
Icarus 1996, 123, 180–191.

[2] Barge, P., and R. Pellat
Mass spectrum and velocity dispersions during planetesimal accumulation. I. Accretion
Icarus 1991 93, 270–287

[3] Philip J. Armitage
Astrophysics of Planet Formation
Sec. 4.5.1, Pg. 131
10 Dec. 2009

[4] K. Tsiganis, R. Gomes, A. Morbidelli and H. F. Levison
Origin of the orbital architecture of the giant planets of the Solar System
Nature, Vol 435, P 469–451, 26 May 2005

[5] Konstantin Batygin and Michael E. Brown
Early Dynamical Evolution of the Solar System: Pinning Down the Initial Conditions of the Nice Model
ApJ, 716:1323–1331, 2010 June 20

[6] Alexander J. Mustill, Sean N. Raymond, and Melvyn B. Davies
Is there an exoplanet in the Solar System?
MNRAS Issue 1, p.109-L113

[7] Maxwell Xu Cai, Simon Portegies Zwart, and Arjen van Elteren
The signatures of the parental cluster on field planetary systems
MNRAS, V. 474, Issue 4, 11 March 2018, Pages 5114–5121

[8] H. Baumgardt
N-body modelling of globular clusters: masses, mass-to-light ratios and intermediate-mass black holes
MNRAS, V. 464, Issue 2, 11 January 2017, P 2174–2202.

[9] Williams, David   https://nssdc.gsfc.nasa.gov/planetary/factsheet/
     TPlanetary Fact Sheet - Metric   As of: December 5, 2018

A   Initial Conditions for Solar System

Planet	Mass (10^{24} kg)	Initial Orbital Velocity ($\mathrm{km\,s^{-1}}$)	Initial Orbital Radius (AU)
Earth	5.97	29.8	1.00
Mars	0.642	24.1	1.41
Jupiter	1898	13.1	5.03
Saturn	568	9.7	9.20
Uranus	86.8	6.8	18.64
Neptune	102	5.4	30.22

Table 2: Initial Conditions taken from [9]

B   Relationship to previous projects

If you have already completed a project in the group where you are working, you should include a $\sim$ 1-page statement indicating how the PHY480 project differs from previous work. This is especially important if you are building on previous work done, for example, during a summer project. You must state clearly the new work that you have done during this semester.